JOURNAL OF GUIDANCE, CONTROL, AND DYNAMICS
Vol. 28, No. 4, July–August 2005

Line-of-Sight Guidance Laws for Formation Flight

Min-Jea Tahk,* Chang-Su Park,† and Chang-Kyung Ryoo†
Korea Advanced Institute of Science and Technology, Daejeon 305-701, Republic of Korea

Two-dimensional formation guidance laws for formation flight using only line-of-sight angle information are addressed. The main idea is to use the line-of-sight angles to two nearby vehicles to maintain the formation position of the current vehicle. Such a formation guidance law is useful because measurement of the line-of-sight angles does not require data communication between the vehicles. We propose two methods of using the line-of-sight angle information for formation guidance: the angle information is used to control the flight-path angle and the velocity of the formation vehicle. Approach guidance and formation guidance of the two leading vehicles are also proposed. Stability of the proposed formation guidance laws is analyzed by using the Jacobian at the equilibrium point. Multiple-vehicle formation flight is simulated to verify the guidance laws proposed.

Introduction

FORMATION flight of manned aerial vehicles is in general visually coordinated by the pilots. The pilots maneuver their aircrafts to align other aircrafts on specific points inside their cockpit. However, continuing formation flight for an extended period of time is a tiresome job for the pilots. Autonomous formation flight relieves the pilots and is also applicable for a group of unmanned aerial vehicles (UAVs) performing complex missions. Recently, NASA used two F-18s to check the feasibility of autonomous formation flight and the aerodynamic energy benefits.[1] Also a study on tight-formation flight of Lockheed C-5 transport models has shown a reduction in power demand that is directly related to extension in range.[2]

To achieve autonomous formation flight, communication is required between the vehicles involved. Depending on the formation control method, some of the vehicle's data are broadcast to the entire group or they are passed on to the adjacent vehicles only. The simplest case involves transmitting only the leader's position to the followers.[2–4] All the vehicles in formation have an independent navigation system to acquire their own position and velocity information. In Ref. 5, a wireless communication network approach to formation control is introduced. It uses mobile nodes that require position and velocity data of each vehicle. Data received from other vehicles are first used to update the receiver's state of formation. Then the modified data are relayed to other vehicles. This reduces the total bandwidth of communications involved in the formation. For rapid formation maneuvers, the use of the leader's Euler data in addition to position and velocity is proposed for better performance.[6] In Ref. 7, a globally stable automatic formation flight control is derived on a formation that requires position, velocity, heading, and leader's input data by the aircrafts.

Because most autonomous formation flight methods require an active communication link between the vehicles, damage to the receiver or the transmitter is critical to mission success. Vehicles with defective sensors are commanded to leave the formation and a reconfiguration of the formation is required.[8,9] Communication delay also affects the formation.[10] Thus, military missions generally prefer low-bandwidth communication and, if possible, radio silence for stealth purposes. Passive detection of another vehicle and maintaining the formation, if possible, would be much preferred to the methods that use two-way data links.

One possible method for passive sensing is to use the wake produced by the leading aircraft.[11] A neural network is used to estimate the relative position from the leader. The initial training phase of the neural network requires the follower to receive a relative position from the leader. Another passive method for sensing the vehicles is to use visual sensors. Vision-based formation control is an actively studied topic in robotics.[12] An omnidirectional visual camera mounted on the robot allows an estimate of a nearby robot's position, velocity, and attitude through an extended Kalman filter. In Ref. 13, an adaptive approach to vision-based UAV formation control assumes that line-of-sight (LOS) range can be estimated by the visual sensors. Each vehicle in formation can measure its speed, heading, LOS range, and angle to other vehicles. The developed formation control assumes that the neighboring vehicles are stationary in formation and dynamic model inversion errors are adaptively approximated by the neural network. In Ref. 14, a computer vision simulation of formation flight using a pose estimation algorithm is done. Five light-emitting diodes placed on the leader are used by the wingman to estimate the leader's position and attitude.

In this paper, we use only the LOS angles to other vehicles measured by visual sensors or radars for multiple-vehicle formation flight. Passive sensing of the data allows for a radio silence formation flight whereas conventional methods require continuous data transfer between the vehicles. Use of LOS angles closely approximates actual birds, which only depend on vision and flow of the wind below their wings to maintain formation. We propose simple guidance laws for approaching and forming the formation. The LOS angles and angular rates are used to control the velocity and heading of the wingmen. Position and velocity data of the nearby vehicles are not required by the following wingmen. The two predetermined LOS formation angles guarantee a unique equilibrium point for the closed-loop system. The guidance gains can be checked for local stability at the equilibrium point.

This paper is organized as follows. In the next section, two-vehicle approach/formation guidance is first introduced. After the first two vehicles are in formation, other vehicles join the formation by using the $\theta-\theta$ guidance, which is introduced next. Equilibrium points and the stability of the closed-loop systems are also studied. Simulation for two, three, and six UAVs converging to a formation is given afterward. Conclusions are provided in the final section.

Problem Statement

We first classify the formation problem into two-vehicle and multiple-vehicle formation guidance because only one LOS angle can be obtained from two-vehicle formation. The formation procedure is done into two stages, the approach and the formation. The approach guidance stage is activated after the wingman has identified the leader. When the wingman has approached the leader at a certain distance, the formation guidance stage is activated. Problem

Received 26 March 2004; accepted for publication 24 May 2004. Copyright © 2004 by the American Institute of Aeronautics and Astronautics, Inc. All rights reserved. Copies of this paper may be made for personal or internal use, on condition that the copier pay the $10.00 per-copy fee to the Copyright Clearance Center, Inc., 222 Rosewood Drive, Danvers, MA 01923; include the code 0731-5090/05 $10.00 in correspondence with the CCC.

*Professor, Division of Aerospace Engineering. Member AIAA.
†Graduate Student, Division of Aerospace Engineering.

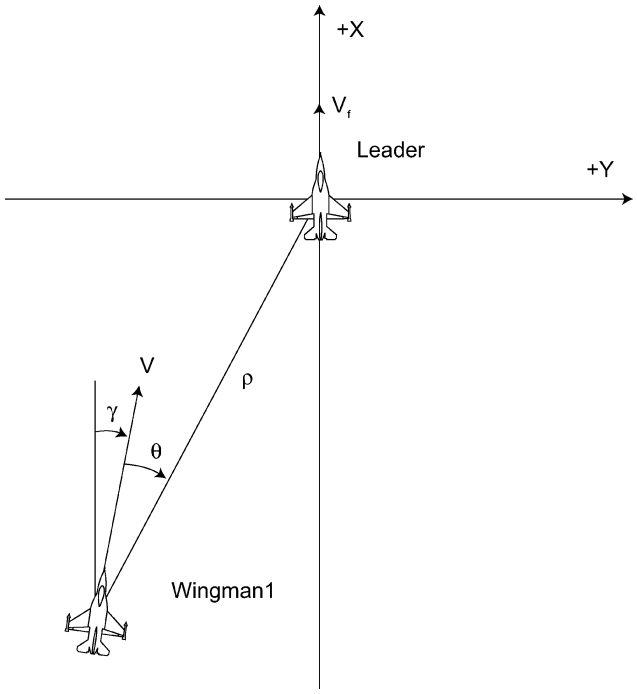

Fig. 1 Two-vehicle guidance geometry.

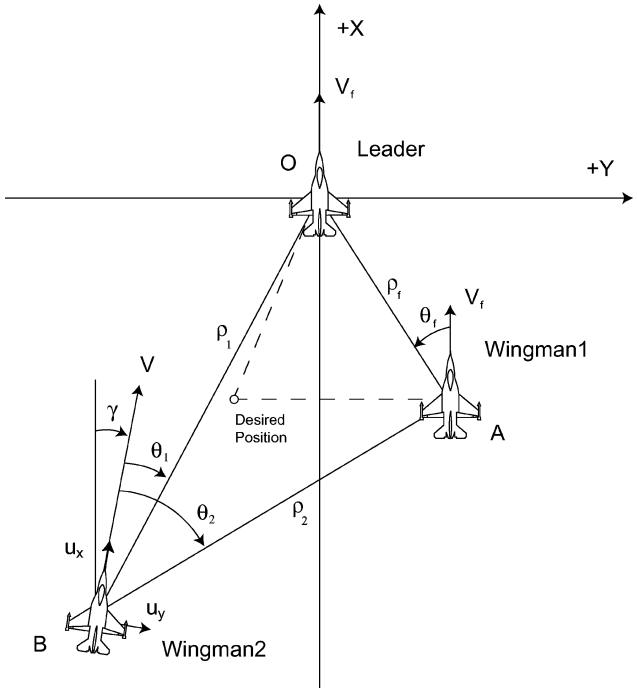

Fig. 2 Three-vehicle guidance geometry.

statements for each case are described as follows. Figures 1 and 2 show the definitions of various angles and distances.

Problem A: Two-Vehicle Formation Guidance

1) Find a guidance law that uses the LOS angle θ and angle rate $\dot{\theta}$ to approach the vehicle at angle θ_c.

2) Find a guidance law that uses the LOS angle θ, LOS angle rate $\dot{\theta}$, relative distance ρ, and relative velocity $\dot{\rho}$ to locate the vehicle at a point specified by θ_c and ρ_c.

Problem B: Multiple-Vehicle Formation Guidance

1) This is the same as that for problem A-1.

2) Find a guidance law that uses the LOS angles θ_1, θ_2 and angle rates $\dot{\theta}_1$, $\dot{\theta}_2$ to locate the vehicle at a point specified by θ_{1c}, θ_{2c}.

Assumptions

Control inputs for the vehicles are the rate of velocity, $\dot{V} = \mathrm{d}V/\mathrm{d}t$, and the rate of flight-path angle, $\dot{\gamma}$.

LOS angles θ_1 and θ_2 are measured with reference to the current vehicle's heading direction.

The leader and wingman 1 are in perfect formation (identical heading and speed) in problem B-2. They are flying in the $+X$ direction.

In this paper, only two-dimensional formation guidance is considered. However, the guidance laws proposed can be extended to three-dimensional formation with some modification.

Two-Vehicle Formation Guidance

The two-vehicle approach and formation guidance are presented in this section. This is a basis for multiple-vehicle formation because the LOS-only guidance proposed requires two LOS angles from two vehicles already in formation.

θ Approach

The simplest way to approach a target vehicle is to use the LOS information only. The LOS angle can be acquired by visual sensors or by radar. The leader may also broadcast a beacon signal for the wingman while the formation forming is in progress. The guidance commands for the wingman are the velocity V and flight-path angle γ.

The θ approach guidance is expressed by

$$\dot{\gamma} = k_1(\theta - \theta_c) + k_2\dot{\theta} \tag{1}$$

$$\dot{V} = \dot{V}_{\max} \tag{2}$$

where θ_c is the commanded LOS angle, $\dot{V}_{\max}$ is the maximum acceleration possible, and k_1 and k_2 are the guidance gains. The velocity is limited by a speed limit, $V_{\max}$. Approach guidance is illustrated in Fig. 1, where the $+X, +Y$ directions are defined. The leader is flying in the $+X$ direction at formation speed V_f. The coordinate frame is fixed to the leader. The positive direction of γ and θ are shown in Fig. 1. For a wingman approaching from the left, The gains are given as $k_1 > 0$ and $k_2 > 0$ for guidance-loop stability. These gain regions allow the wingman to turn counterclockwise to match the commanded LOS angle when the current LOS angle is smaller than the commanded one. The $\dot{\theta}$ term of Eq. (1) is included as a damping term in the guidance law.

$\rho-\theta$ Guidance

A single LOS angle θ_c just specifies a line on which the wingman should locate. Additional information is required to direct the wingman to a specific point on the line. For two-vehicle formation with one leader and one wingman, we use the relative distance ρ as the additional information. The relative distance information is also assumed to be obtained from visual sensors or radar.

The following feedback laws are used for the $\rho-\theta$ guidance of this study:

$$\dot{\gamma} = k_1(\theta - \theta_c) + k_2\dot{\theta} \tag{3}$$

$$\dot{V} = k_3(\rho - \rho_c) + k_4\dot{\rho} \tag{4}$$

For the preceding θ approach, the velocity is simply increased until the speed limit is reached. However, for the $\rho-\theta$ guidance, the velocity command is controlled by the relative distance information. In Eq. (4), ρ_c is the commanded formation distance and $k_3 > 0$ so that the velocity is increased if the current distance is larger than the commanded distance.

Multiple-Vehicle Formation Guidance

After the two vehicles have formed a "perfect formation" by previous guidance laws, the vehicles provide two different LOS angles that can be acquired by other approaching wingmen.

In this section, two LOS-only formation guidance laws are proposed. The guidance laws and kinematic equation for the formation

are first derived. The unique equilibrium point is obtained for each guidance law. The stability of the guidance laws is then analyzed by linearizing the nonlinear formation dynamics at the equilibrium point.

$\theta-\theta$ Guidance Law 1

The $\theta-\theta$ guidance law proposed first is similar in form to the $\rho-\theta$ guidance law. The flight-path angle rate $\dot{\gamma}$ of wingman 2 is controlled by θ_1, which is the LOS angle to the leader. The velocity is controlled by θ_2, which is the LOS angle to wingman 1. This $\theta-\theta$ guidance law can be expressed as

$$\dot{\gamma} = k_1(\theta_1 - \theta_{1c}) + k_2\dot{\theta}_1 \tag{5}$$

$$\dot{V} = k_3(\theta_2 - \theta_{2c}) + k_4\dot{\theta}_2 \tag{6}$$

The desired formation position for wingman 2 is determined by the intersection of the two lines dictated by θ_{1c} and θ_{2c}.

$\theta-\theta$ Guidance Law 2

The second $\theta-\theta$ guidance law proposed uses the sum and difference of the two LOS angle errors and two LOS angle rates, which are defined as

$$\Delta\theta^+ \triangleq (\theta_1 - \theta_{1c}) + (\theta_2 - \theta_{2c}) \tag{7}$$

$$\Delta\theta^- \triangleq (\theta_1 - \theta_{1c}) - (\theta_2 - \theta_{2c}) \tag{8}$$

$$\dot{\theta}^+ \triangleq \dot{\theta}_1 + \dot{\theta}_2 \tag{9}$$

$$\dot{\theta}^- \triangleq \dot{\theta}_1 - \dot{\theta}_2 \tag{10}$$

We define the reference line θ_{ref} as

$$\theta_{\text{ref}} = (\theta_{1c} + \theta_{2c})/2 \tag{11}$$

Then, with respect to the reference line, the tangential acceleration a_t and radial acceleration a_r are commanded as

$$a_t = -k_p\Delta\theta^+ - k_d\dot{\theta}^+ \tag{12}$$

$$a_r = -k_p\Delta\theta^- - k_d\dot{\theta}^- \tag{13}$$

By using the coordinate transformation, we obtain

$$\dot{\gamma} = u_y/V_0 = (k_g/V_0)a_y = (k_g/V_0)(-a_t\cos\theta_{\text{ref}} - a_r\sin\theta_{\text{ref}}) \tag{14}$$

$$\dot{V} = u_x = k_v a_x = k_v(a_t\sin\theta_{\text{ref}} - a_r\cos\theta_{\text{ref}}) \tag{15}$$

where V_0 is the initial velocity of wingman 2; a_x and a_y are the acceleration commands in the direction of u_x and u_y in Fig. 2; and k_p, k_d, k_g, and k_v are feedback gains.

Substituting Eqs. (7–13) into Eqs. (14) and (15) gives

$$\dot{\gamma} = (k_g/V_0)\Big[-\left(-k_p\Delta\theta^+ - k_d\dot{\theta}^+\right)\cos\theta_{\text{ref}} - \left(-k_p\Delta\theta^- - k_d\dot{\theta}^-\right)\sin\theta_{\text{ref}}\Big] \tag{16}$$

$$= (k_g/V_0)\Big\{k_p\cos\theta_{\text{ref}}[(\theta_1 - \theta_{1c}) + (\theta_2 - \theta_{2c})] + k_d\cos\theta_{\text{ref}}(\dot{\theta}_1 + \dot{\theta}_2) + k_p\sin\theta_{\text{ref}}[(\theta_1 - \theta_{1c}) - (\theta_2 - \theta_{2c})] + k_d\sin\theta_{\text{ref}}(\dot{\theta}_1 - \dot{\theta}_2)\Big\} \tag{17}$$

$$= (k_g k_p/V_0)(\cos\theta_{\text{ref}} + \sin\theta_{\text{ref}})(\theta_1 - \theta_{1c}) + (k_g k_p/V_0) \times(\cos\theta_{\text{ref}} - \sin\theta_{\text{ref}})(\theta_2 - \theta_{2c}) + (k_g k_d/V_0) \times(\cos\theta_{\text{ref}} + \sin\theta_{\text{ref}})\dot{\theta}_1 + (k_g k_d/V_0)(\cos\theta_{\text{ref}} - \sin\theta_{\text{ref}})\dot{\theta}_2 \tag{18}$$

$$\dot{V} = k_v\Big[\left(-k_p\Delta\theta^+ - k_d\dot{\theta}^+\right)\sin\theta_{\text{ref}} - \left(-k_p\Delta\theta^- - k_d\dot{\theta}^-\right)\cos\theta_{\text{ref}}\Big] \tag{19}$$

$$= k_v\Big\{-k_p\sin\theta_{\text{ref}}[(\theta_1 - \theta_{1c}) + (\theta_2 - \theta_{2c})] - k_d\sin\theta_{\text{ref}}(\dot{\theta}_1 + \dot{\theta}_2) + k_p\cos\theta_{\text{ref}}[(\theta_1 - \theta_{1c}) - (\theta_2 - \theta_{2c})] + k_d\cos\theta_{\text{ref}}(\dot{\theta}_1 - \dot{\theta}_2)\Big\} \tag{20}$$

$$= k_v k_p(-\sin\theta_{\text{ref}} + \cos\theta_{\text{ref}})(\theta_1 - \theta_{1c}) - k_v k_p(\sin\theta_{\text{ref}} + \cos\theta_{\text{ref}}) \times(\theta_2 - \theta_{2c}) + k_v k_d(-\sin\theta_{\text{ref}} + \cos\theta_{\text{ref}})\dot{\theta}_1 - k_v k_d(\sin\theta_{\text{ref}} + \cos\theta_{\text{ref}})\dot{\theta}_2 \tag{21}$$

We define new variables as follows:

$$k_{gp1} = (k_g k_p/V_0)(\sin\theta_{\text{ref}} + \cos\theta_{\text{ref}}) \tag{22}$$

$$k_{gp2} = (k_g k_p/V_0)(-\sin\theta_{\text{ref}} + \cos\theta_{\text{ref}}) \tag{23}$$

$$k_{gd1} = (k_g k_d/V_0)(\sin\theta_{\text{ref}} + \cos\theta_{\text{ref}}) \tag{24}$$

$$k_{gd1} = (k_g k_d/V_0)(-\sin\theta_{\text{ref}} + \cos\theta_{\text{ref}}) \tag{25}$$

$$k_{vp1} = k_v k_p(-\sin\theta_{\text{ref}} + \cos\theta_{\text{ref}}) \tag{26}$$

$$k_{vp2} = -k_v k_p(\sin\theta_{\text{ref}} + \cos\theta_{\text{ref}}) \tag{27}$$

$$k_{vd1} = k_v k_d(-\sin\theta_{\text{ref}} + \cos\theta_{\text{ref}}) \tag{28}$$

$$k_{vd2} = -k_v k_d(\sin\theta_{\text{ref}} + \cos\theta_{\text{ref}}) \tag{29}$$

Applying the newly defined variables to Eqs. (18) and (21), we obtain the following $\theta-\theta$ guidance law:

$$\dot{\gamma} = k_{gp1}(\theta_1 - \theta_{1c}) + k_{gp2}(\theta_2 - \theta_{2c}) + k_{gd1}\dot{\theta}_1 + k_{gd2}\dot{\theta}_2 \tag{30}$$

$$\dot{V} = k_{vp1}(\theta_1 - \theta_{1c}) + k_{vp2}(\theta_2 - \theta_{2c}) + k_{vd1}\dot{\theta}_1 + k_{vd2}\dot{\theta}_2 \tag{31}$$

Being different from the first $\theta-\theta$ guidance law, both γ and V are controlled by using the information on θ_1 and θ_2.

Kinematic Equation for Formation Flight

To analyze the proposed $\theta-\theta$ guidance laws, we first derive the kinematic equation for formation flight. From the three-vehicle formation geometry shown in Fig. 2, we define

$$\Delta V_x = V\cos\gamma - V_f \tag{32}$$

$$\Delta V_y = V\sin\gamma \tag{33}$$

where ΔV_x and ΔV_y are the velocity difference between wingman 2 and the leader in the X and Y directions, respectively. If the formation distance ρ_f and formation angle θ_f between the leader and wingman 1 are given, the distance from wingman 2 to the other vehicles can be found from the law of sine:

$$\rho_1 = \rho_f\left|\frac{\sin(\gamma + \theta_2 + \theta_f)}{\sin(\theta_2 - \theta_1)}\right| \tag{34}$$

$$\rho_2 = \rho_f\left|\frac{\sin(\gamma + \theta_1 + \theta_f)}{\sin(\theta_2 - \theta_1)}\right| \tag{35}$$

where ρ_1 is the distance between the leader and wingman 2, and ρ_2 is the distance between wingman 1 and wingman 2.

From Fig. 2, we can show that

$$\frac{\mathrm{d}}{\mathrm{d}t}(\gamma+\theta_1)=\frac{1}{\rho_1}[\Delta V_x\sin(\gamma+\theta_1)-\Delta V_y\cos(\gamma+\theta_1)] \quad (36)$$

$$\dot{\theta}_1=\frac{1}{\rho_1}[\Delta V_x\sin(\gamma+\theta_1)-\Delta V_y\cos(\gamma+\theta_1)]-\dot{\gamma} \quad (37)$$

Similarly, we have

$$\dot{\theta}_2=(1/\rho_2)[\Delta V_x\sin(\gamma+\theta_2)-\Delta V_y\cos(\gamma+\theta_2)]-\dot{\gamma} \quad (38)$$

Substituting Eqs. (32) and (33) into Eqs. (37) and (38) gives

$$\dot{\theta}_1=(1/\rho_1)[(V\cos\gamma-V_f)\sin(\gamma+\theta_1) - V\sin\gamma\cos(\gamma+\theta_1)]-\dot{\gamma} \quad (39)$$

$$=(1/\rho_1)[V\sin(\gamma+\theta_1-\gamma)-V_f\sin(\gamma+\theta_1)]-\dot{\gamma} \quad (40)$$

$$=(1/\rho_1)[V\sin\theta_1-V_f\sin(\gamma+\theta_1)]-\dot{\gamma} \quad (41)$$

$$\dot{\theta}_2=(1/\rho_2)[V\sin\theta_2-V_f\sin(\gamma+\theta_2)]-\dot{\gamma} \quad (42)$$

Stability Analysis for $\theta-\theta$ Guidance Law 1

To verify the stability of the proposed formation guidance law, we proceed in the following order. First, the related equations are rearranged into matrices. Then the equilibrium point that satisfies the nonlinear equations is found. The Jacobian matrix is then found for the given equilibrium point. If the eigenvalues of the Jacobian matrix are all located on the left half-plane, the system is stable for the equilibrium point. Analysis is first performed on $\theta-\theta$ guidance law 1.

Guidance law equations, Eqs. (5) and (6), and kinematic equations, Eqs. (41) and (42), are rearranged as

$$\dot{\theta}_1+\dot{\gamma}=(1/\rho_1)[V\sin\theta_1-V_f\sin(\gamma+\theta_1)] \quad (43)$$

$$\dot{\theta}_2+\dot{\gamma}=(1/\rho_2)[V\sin\theta_2-V_f\sin(\gamma+\theta_2)] \quad (44)$$

$$-k_2\dot{\theta}_1+\dot{\gamma}=k_1(\theta_1-\theta_{1c}) \quad (45)$$

$$-k_4\dot{\theta}_2+\dot{V}=k_3(\theta_2-\theta_{2c}) \quad (46)$$

The preceding equations can be rewritten as the following matrix equations:

$$\begin{pmatrix}1&0&1&0\\0&1&1&0\\-k_2&0&1&0\\0&-k_4&0&1\end{pmatrix}\begin{pmatrix}\dot{\theta}_1\\\dot{\theta}_2\\\dot{\gamma}\\\dot{V}\end{pmatrix}=\begin{pmatrix}\frac{1}{\rho_1}[V\sin\theta_1-V_f\sin(\gamma+\theta_1)]\\\frac{1}{\rho_2}[V\sin\theta_2-V_f\sin(\gamma+\theta_2)]\\k_1(\theta_1-\theta_{1c})\\k_3(\theta_2-\theta_{2c})\end{pmatrix} \quad (47)$$

Performing matrix inversion, we have

$$\begin{pmatrix}\dot{\theta}_1\\\dot{\theta}_2\\\dot{\gamma}\\\dot{V}\end{pmatrix}=\begin{pmatrix}\frac{1}{1+k_2}&0&-\frac{1}{1+k_2}&0\\-\frac{k_2}{1+k_2}&1&-\frac{1}{1+k_2}&0\\\frac{k_2}{1+k_2}&0&\frac{1}{1+k_2}&0\\-\frac{k_2k_4}{1+k_2}&\frac{k_4+k_2k_4}{1+k_2}&-\frac{k_4}{1+k_2}&1\end{pmatrix}\times\begin{pmatrix}\frac{1}{\rho_1}[V\sin\theta_1-V_f\sin(\gamma+\theta_1)]\\\frac{1}{\rho_2}[V\sin\theta_2-V_f\sin(\gamma+\theta_2)]\\k_1(\theta_1-\theta_{1c})\\k_3(\theta_2-\theta_{2c})\end{pmatrix} \quad (48)$$

Equation (48) is the formation kinematics with $\theta-\theta$ guidance law 1 input.

We now find the equilibrium point for Eq. (48). Equilibrium points should satisfy

$$\begin{pmatrix}\frac{1}{1+k_2}&0&-\frac{1}{1+k_2}&0\\-\frac{k_2}{1+k_2}&1&-\frac{1}{1+k_2}&0\\\frac{k_2}{1+k_2}&0&\frac{1}{1+k_2}&0\\-\frac{k_2k_4}{1+k_2}&\frac{k_4+k_2k_4}{1+k_2}&-\frac{k_4}{1+k_2}&1\end{pmatrix}\times\begin{pmatrix}\frac{1}{\rho_1}\left[V\sin\theta_1-V_f\sin(\gamma+\theta_1)\right]\\\frac{1}{\rho_2}\left[V\sin\theta_2-V_f\sin(\gamma+\theta_2)\right]\\k_1(\theta_1-\theta_{1c})\\k_3(\theta_2-\theta_{2c})\end{pmatrix}=0 \quad (49)$$

Since all gains can be chosen arbitrarily, the equation reduces to

$$(1/\rho_1)[V\sin\theta_1-V_f\sin(\gamma+\theta_1)]=0 \quad (50)$$

$$(1/\rho_2)[V\sin\theta_2-V_f\sin(\gamma+\theta_2)]=0 \quad (51)$$

$$k_1(\theta_1-\theta_{1c})=0 \quad (52)$$

$$k_3(\theta_2-\theta_{2c})=0 \quad (53)$$

where θ_{1c} and θ_{2c} are the equilibrium points of θ_1 and θ_2 from Eqs. (52) and (53). Inputting these values into Eqs. (50) and (51), we have

$$V\sin\theta_{1c}-V_f\sin(\gamma+\theta_{1c})=0 \quad (54)$$

$$V\sin\theta_{2c}-V_f\sin(\gamma+\theta_{2c})=0 \quad (55)$$

Applying [Eq. (54)] $\times\ \sin(\gamma+\theta_{2c})-$ [Eq. (55)] $\times\ \sin(\gamma+\theta_{1c})$,

$$V[\sin\theta_{1c}\sin(\gamma+\theta_{2c})-\sin\theta_{2c}\sin(\gamma+\theta_{1c})]=0 \quad (56)$$

Then $\gamma=0$ since $\theta_{1c}\neq\theta_{2c}$ in general and $V=V_f$. Therefore, $[\theta_{1c},\theta_{2c},0,V_f]$ is the unique equilibrium point of this system. If the system is stable for this point, the guidance will generally guide the vehicle to this unique point.

We now find the Jacobian matrix by linearizing the system at the equilibrium point.

Let $A=(\partial f/\partial x)(x)\big|_{x=x_e}$, where

$$x=[\theta_1,\theta_2,\gamma,V]^T \quad (57)$$

$$x_e=[\theta_{1c},\theta_{2c},0,V_f]^T \quad (58)$$

Here f is the result given after multiplication of the matrices on the right-hand side of Eq. (48). After tedious calculations, Jacobian matrix A is given as

$$A = \begin{pmatrix} -\dfrac{k_1}{1+k_2} & 0 & -\dfrac{V_f \cos\theta_{1c}}{(1+k_2)\tilde{\rho}_1} & \dfrac{\sin\theta_{1c}}{(1+k_2)\tilde{\rho}_1} \\ -\dfrac{k_1}{1+k_2} & 0 & \dfrac{k_2 V_f \cos\theta_{1c}}{(1+k_2)\tilde{\rho}_1} - \dfrac{V_f \cos\theta_{2c}}{\tilde{\rho}_2} & -\dfrac{k_2 \sin\theta_{1c}}{(1+k_2)\tilde{\rho}_1} + \dfrac{\sin\theta_{2c}}{\tilde{\rho}_2} \\ \dfrac{k_1}{1+k_2} & 0 & -\dfrac{k_2 V_f \cos\theta_{1c}}{(1+k_2)\tilde{\rho}_1} & \dfrac{k_2 \sin\theta_{1c}}{(1+k_2)\tilde{\rho}_1} \\ -\dfrac{k_1 k_4}{1+k_2} & k_3 & \dfrac{k_2 k_4 V_f \cos\theta_{1c}}{(1+k_2)\tilde{\rho}_1} - \dfrac{k_4 V_f \cos\theta_{2c}}{\tilde{\rho}_2} & -\dfrac{k_2 k_4 \sin\theta_{1c}}{(1+k_2)\tilde{\rho}_1} + \dfrac{k_4 \sin\theta_{2c}}{\tilde{\rho}_2} \end{pmatrix} \tag{59}$$

where

$$\tilde{\rho}_1 = \rho_f \frac{\sin(\theta_{2c} + \theta_f)}{\sin(\theta_{2c} - \theta_{1c})} \tag{60}$$

$$\tilde{\rho}_2 = \rho_f \frac{\sin(\theta_{1c} + \theta_f)}{\sin(\theta_{2c} - \theta_{1c})} \tag{61}$$

The $\tilde{\rho}_1$ and $\tilde{\rho}_2$ are the values of ρ_1 and ρ_2 at the equilibrium point.

The characteristic equation can be found by

$$\det(sI - A) = 0 \tag{62}$$

To check the closed-loop stability of the system, we can find the eigenvalues of the system for given guidance gains. If the eigenvalues are located on the left half-plane it is a stable system near the equilibrium point.

Stability Analysis for $\theta-\theta$ Guidance Law 2

We apply the same stability analysis approach for $\theta-\theta$ guidance law 2. The guidance law equations, Eqs. (30) and (31), and the kinematic equations, Eqs. (41) and (42), are rearranged as follows:

$$\dot{\theta}_1 + \dot{\gamma} = (1/\rho_1)[V \sin\theta_1 - V_f \sin(\gamma + \theta_1)] \tag{63}$$

$$\dot{\theta}_2 + \dot{\gamma} = (1/\rho_2)[V \sin\theta_2 - V_f \sin(\gamma + \theta_2)] \tag{64}$$

$$-k_{gd1}\dot{\theta}_1 - k_{gd2}\dot{\theta}_2 + \dot{\gamma} = k_{gp1}(\theta_1 - \theta_{1c}) + k_{gp2}(\theta_2 - \theta_{2c}) \tag{65}$$

$$-k_{vd1}\dot{\theta}_1 - k_{vd2}\dot{\theta}_2 + \dot{V} = k_{vp1}(\theta_1 - \theta_{1c}) + k_{vp2}(\theta_2 - \theta_{2c}) \tag{66}$$

The preceding equations can be rewritten as

$$\begin{pmatrix} 1 & 0 & 1 & 0 \\ 0 & 1 & 1 & 0 \\ -k_{gd1} & -k_{gd2} & 1 & 0 \\ -k_{vd1} & -k_{vd2} & 0 & 1 \end{pmatrix} \begin{pmatrix} \dot{\theta}_1 \\ \dot{\theta}_2 \\ \dot{\gamma} \\ \dot{V} \end{pmatrix}$$

$$= \begin{pmatrix} \dfrac{1}{\rho_1}[V \sin\theta_1 - V_f \sin(\gamma + \theta_1)] \\ \dfrac{1}{\rho_2}[V \sin\theta_2 - V_f \sin(\gamma + \theta_2)] \\ k_{gp1}(\theta_1 - \theta_{1c}) + k_{gp2}(\theta_2 - \theta_{2c}) \\ k_{vp1}(\theta_1 - \theta_{1c}) + k_{vp2}(\theta_2 - \theta_{2c}) \end{pmatrix} \tag{67}$$

Performing matrix inversion, we obtain

$$\begin{pmatrix} \dot{\theta}_1 \\ \dot{\theta}_2 \\ \dot{\gamma} \\ \dot{V} \end{pmatrix}$$

$$= \frac{1}{\Delta} \begin{pmatrix} 1 + k_{gd2} & -k_{gd2} & -1 & 0 \\ \cdots\cdots & \cdots\cdots & \cdots\cdots & \cdots\cdots \\ -k_{gd1} & 1 + k_{gd1} & -1 & 0 \\ \cdots\cdots & \cdots\cdots & \cdots\cdots & \cdots\cdots \\ k_{gd1} & k_{gd2} & 1 & 0 \\ \cdots\cdots & \cdots\cdots & \cdots\cdots & \cdots\cdots \\ k_{vd1} + k_{gd2}k_{vd1} & -k_{gd2}k_{vd1} + k_{vd2} & & \\ -k_{gd1}k_{vd2} & +k_{gd1}k_{vd2} & -k_{vd1} - k_{vd2} & \Delta \end{pmatrix}$$

$$\times \begin{pmatrix} \dfrac{1}{\rho_1}[V \sin\theta_1 - V_f \sin(\gamma + \theta_1)] \\ \dfrac{1}{\rho_2}[V \sin\theta_2 - V_f \sin(\gamma + \theta_2)] \\ k_{gp1}(\theta_1 - \theta_{1c}) + k_{gp2}(\theta_2 - \theta_{2c}) \\ k_{vp1}(\theta_1 - \theta_{1c}) + k_{vp2}(\theta_2 - \theta_{2c}) \end{pmatrix} \tag{68}$$

where $\Delta = 1 + k_{gd1} + k_{gd2}$. Equation (68) is the dynamics of the guidance loop with $\theta - \theta$ guidance law 2.

Finding the equilibrium point that satisfies

$$\begin{pmatrix} \dfrac{1}{\rho_1}[V \sin\theta_1 - V_f \sin(\gamma + \theta_1)] \\ \dfrac{1}{\rho_2}[V \sin\theta_2 - V_f \sin(\gamma + \theta_2)] \\ k_{gp1}(\theta_1 - \theta_{1c}) + k_{gp2}(\theta_2 - \theta_{2c}) \\ k_{vp1}(\theta_1 - \theta_{1c}) + k_{vp2}(\theta_2 - \theta_{2c}) \end{pmatrix} = 0 \tag{69}$$

for arbitrary gains, we have the same equilibrium point as in formation guidance law 1. Let $[\theta_{1c}, \theta_{2c}, 0, V_f]$ be the unique equilibrium point of this system. Then the Jacobian matrix is given by

$$A = \frac{1}{\Delta}\begin{pmatrix} -k_{gp1} & -k_{gp2} & -(1+k_{gd2})\dfrac{V_f\cos\theta_{1c}}{\tilde{\rho}_1} + k_{gd2}\dfrac{V_f\cos\theta_{2c}}{\tilde{\rho}_2} & (1+k_{gd2})\dfrac{\sin\theta_{1c}}{\tilde{\rho}_1} - k_{gd2}\dfrac{\sin\theta_{2c}}{\tilde{\rho}_2} \\ -k_{gp1} & -k_{gp2} & k_{gd2}\dfrac{V_f\cos\theta_{1c}}{\tilde{\rho}_1} - (1+k_{gd2})\dfrac{V_f\cos\theta_{2c}}{\tilde{\rho}_2} & k_{gd1}\dfrac{\sin\theta_{1c}}{\tilde{\rho}_1} + (1+k_{gd2})\dfrac{\sin\theta_{2c}}{\tilde{\rho}_2} \\ k_{gp1} & k_{gp2} & -k_{gd1}\dfrac{V_f\cos\theta_{1c}}{\tilde{\rho}_1} - k_{gd2}\dfrac{V_f\cos\theta_{2c}}{\tilde{\rho}_2} & k_{gd1}\dfrac{\sin\theta_{1c}}{\tilde{\rho}_1} + k_{gd2}\dfrac{\sin\theta_{2c}}{\tilde{\rho}_2} \\ -k_{gp1}k_{vd1} & -k_{gp2}k_{vd1} & -(k_{vd1}+k_{gd2}k_{vd1}-k_{gd1}k_{vd2})\dfrac{V_f\cos\theta_{1c}}{\tilde{\rho}_1} & (k_{vd1}+k_{gd2}k_{vd1}-k_{gd1}k_{vd2})\dfrac{\sin\theta_{1c}}{\tilde{\rho}_1} \\ -k_{gp1}k_{vd2}+k_{vp1}\Delta & -k_{gp2}k_{vd2}+k_{vp2}\Delta & -(-k_{gd2}k_{vd1}+k_{vd2}+k_{gd1}k_{vd2})\dfrac{V_f\cos\theta_{2c}}{\tilde{\rho}_2} & +(-k_{gd2}k_{vd1}+k_{vd2}+k_{gd1}k_{vd2})\dfrac{\sin\theta_{2c}}{\tilde{\rho}_2} \end{pmatrix} \tag{70}$$

Stability of the closed-loop system can be checked by finding the eigenvalues as in guidance law 1.

We have shown that the proposed guidance laws have a unique equilibrium point, that is common to both of the two guidance laws. This equilibrium point can be checked for local stability for given gains.

Simulation and Discussion

The proposed guidance laws are applied to formation flight simulation for verification. Three cases of simulation are investigated. The first case is a two-vehicle θ approach and $\rho-\theta$ guidance. The second is a three-vehicle $\theta-\theta$ guidance that compares the two proposed guidance laws. The final case is a six-vehicle formation flight to check the applicability of $\theta-\theta$ guidance for N vehicles.

Case 1: θ Approach and $\rho-\theta$ Guidance

The θ approach and $\rho-\theta$ guidance are applied to a two-vehicle formation flight. The initial position of the leader is $X_1(0) = (0, 0)$ and of the wingman is $X_2(0) = (-5000, -5000)$. The initial velocity for all vehicles is $V_i = (100, 0)$. The leader vehicle flies on a straight path and the wingman tracks and approaches the leader using the θ approach. When the wingman is inside the formation guidance activation region, which is set to 500, the wingman switches to $\rho-\theta$ guidance. The target relative position of the wingman is set to $(-30, 30)$ with respect to the leader. For this formation geometry, the commanded angle θ_c is -45 deg and the commanded distance ρ_c is $30\sqrt{2}$.

The vehicles involved are limited by the following constraints:

$$V_{\max} = 150, \qquad V_{\min} = 80 \tag{71}$$

$$|\dot{V}|_{\max} = 10, \qquad |\dot{\gamma}|_{\max} = 0.1 \text{ rad/s} \tag{72}$$

The simulation is done for 250 s with time step of 0.1 s. The gains are set to $k_1 = 0.2$ and $k_2 = 0.2$ for θ approach. For $\rho-\theta$ guidance, gains are set to $k_1 = 0.02$, $k_2 = 0.2$, $k_3 = 0.05$, and $k_4 = 0.2$.

Figures 3 and 4 show the simulation results. Figure 3 is the plot of relative distance from the leader. The leader is marked as a triangle on $(0, 0)$. The wingman starts from $(-5000, -5000)$, which is on the bottom left. The approach angle command θ_c is given as -5, 0, and 5 deg to see if the approach guidance makes the vehicles approach in the desired angles. Figure 4 is the magnified view of Fig. 3 near the leader. The approach guidance gives a distinct approach angle

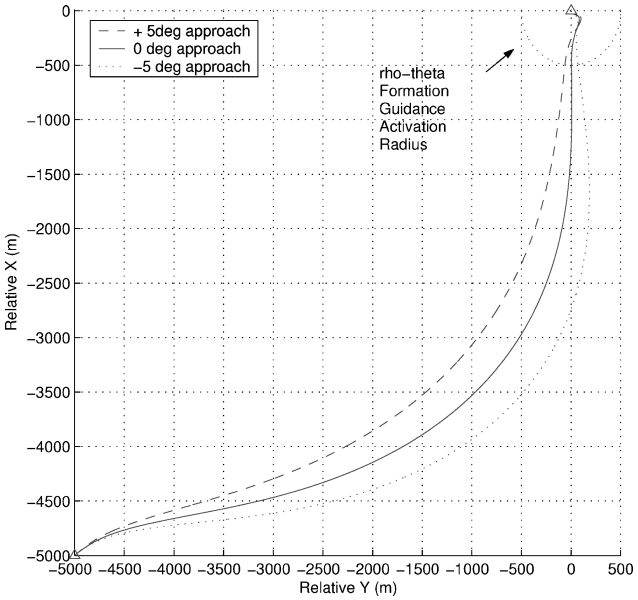

Fig. 3 Case 1: relative $X-Y$.

when nearing the leader. Entering the $\rho-\theta$ guidance region, the vehicles converge to the commanded formation location. The case of the +5 deg approach is the first to enter the region at around 115 s because the distance required to travel is the shortest.

The simulation results show that θ approach plus $\rho-\theta$ guidance works well in forming a two-vehicle formation. This formation is the basis for $\theta-\theta$ guidance.

Case 2: $\theta-\theta$ Guidance

The $\theta-\theta$ guidance is applied to a three-vehicle formation flight. The initial position of the leader is $X_1(0) = (0, 0)$, of wingman 1 is $X_2(0) = (-30, 30)$, and of wingman 2 is $X_3(0) = (-50, -50)$. Initial velocities for all vehicles are $V_i(0) = (100, 0)$. The leader and wingman 1 are in perfect formation, flying a straight path, and wingman 2 moves into the desired formation position by the guidance law. The target location of wingman 2 is set to $(-30, -30)$ from the leader. Then commanded angle 1, θ_{1c}, is 45 deg and commanded angle 2, θ_{2c}, is 90 deg.

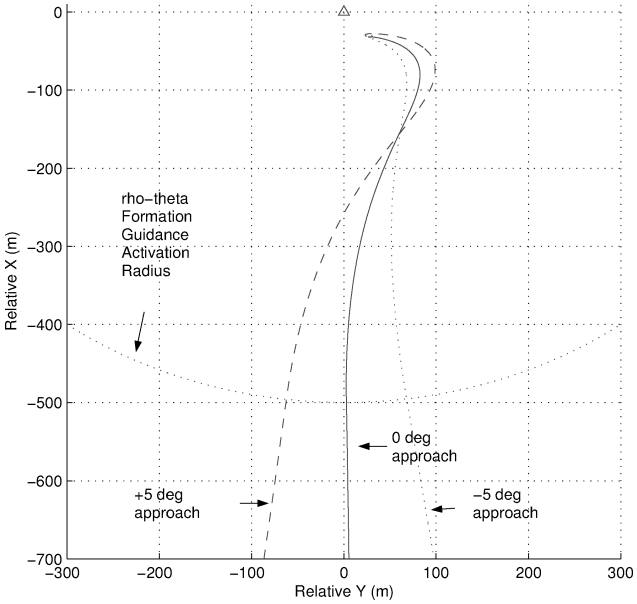

Fig. 4 Case 1: relative $X-Y$ magnified.

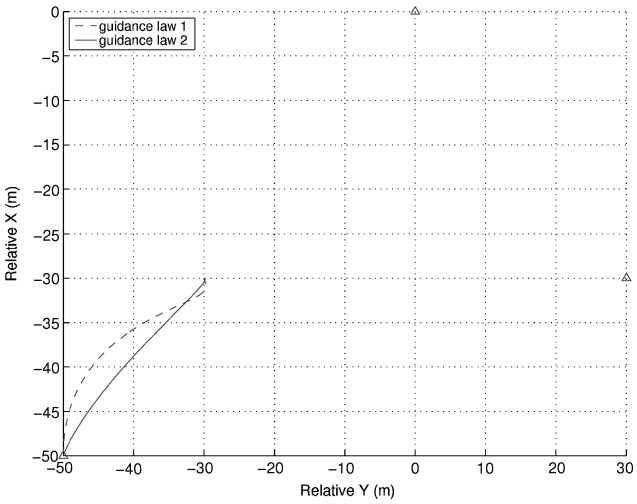

Fig. 5 Case 2: relative $X-Y$.

The simulation is done for 100 s with a time step of 0.1 s. The gains are set to $k_1 = 0.02$, $k_2 = 0.2$, $k_3 = -20$, and $k_4 = -200$ for $\theta-\theta$ guidance law 1. To check the stability of the system for this gain set, we input the gains and the formation conditions into Eq. (59). The eigenvalues for the Jacobian matrix are

$$-2.63029, \qquad -0.169358 \pm 0.0736389i, \qquad -0.103218 \quad (73)$$

Because the eigenvalues are all located on the left half-plane, the system with guidance law 1 is stable for this gain set.

Gains for $\theta-\theta$ guidance law 2 are set to $k_p = 1$, $k_d = 5$, $k_v = 10$, and $k_g = 10$; θ_{ref} for case 2 is $3\pi/8$. Then, calculating Eqs. (22–29), we have $k_{gp1} = 0.1307$, $k_{gp2} = -0.0541$, $k_{gd1} = 0.6533$, $k_{gd2} = -0.2706$, $k_{vp1} = -5.4120$, $k_{vp2} = -13.0656$, $k_{vd1} = -27.0598$, and $k_{vd2} = -65.3281$. Applying these gains to Eq. (70), we obtain the eigenvalues

$$-0.696008 \pm 0.193973i, \qquad -0.333974, \qquad -0.230451 \quad (74)$$

All the eigenvalues are located on the left half-plane, where the system with guidance law 2 is stable for this gain set.

Simulation results are shown in Figs. 5–7. Figure 5 is a relative distance plot for $\theta-\theta$ guidance laws 1 and 2. The dashed line is law 1 and the solid line is law 2. The leader is marked as a triangle on $(0, 0)$ and wingman 1 is at $(-30, 30)$. Both guidance laws guide the vehicle to the desire LOS angle as seen in Fig. 6. Guidance law 2 shows a faster settling time than guidance law 1 for the given gain set.

Table 1 Six-vehicle formation initial location and target location

Vehicle no.	Initial X	Initial Y	Target X	Target Y
1 (leader)	0	0	0	0
2	−30	30	−30	30
3	−5000	−5000	−30	−30
4	−6000	−6000	−60	0
5	−7000	−7000	−60	60
6	−8000	−8000	−60	−60

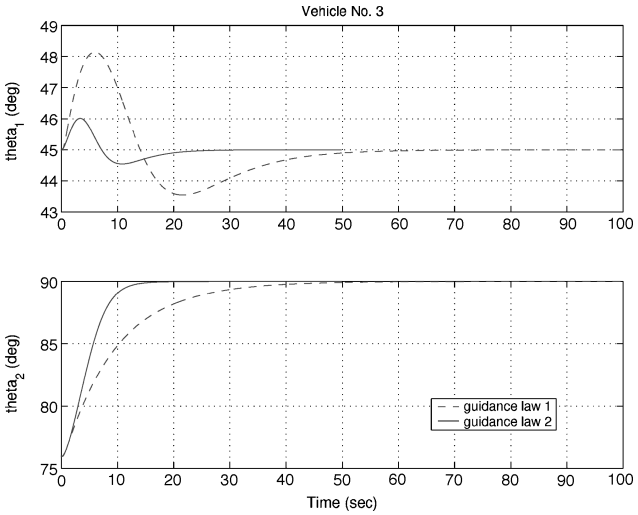

Fig. 6 Case 2: θ_1 and θ_2.

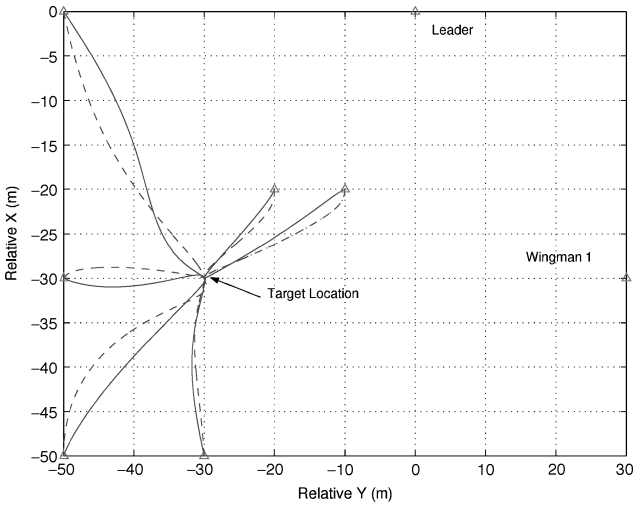

Fig. 7 $\theta-\theta$ guidance law comparison plot for various conditions.

The two guidance laws are also tested for various initial conditions: $(-50, -50)$, $(-30, -50)$, $(-50, -30)$, $(0, -50)$, $(-20, -20)$, and $(-20, -10)$ are given as the wingman 2's initial location. Figure 7 shows the results for law 1 (dashed line) and law 2 (solid line). Both guidance laws are successful in making the vehicle form a formation with only LOS angle information.

Case 3: Six-Vehicle $\theta-\theta$ Guidance

For the final case, a six-vehicle approach with $\theta-\theta$ guidance is simulated. The initial position and the target position of the vehicles involved are given in Table 1. The initial velocities for all the vehicles are $V_i(0) = (100, 0)$. The leader and wingman 1 are in perfect formation, flying a straight path, and other wingmen move into the

Table 2 Six-vehicle formation angle commands

Vehicle no.	Target vehicle 1	θ_{1c}, deg	Target vehicle 2	θ_{2c}, deg	Approach angle, deg
3	1	+45	2	+90	+5
4	2	+45	3	−45	0
5	2	−45	4	−90	−5
6	3	+45	4	+90	+5

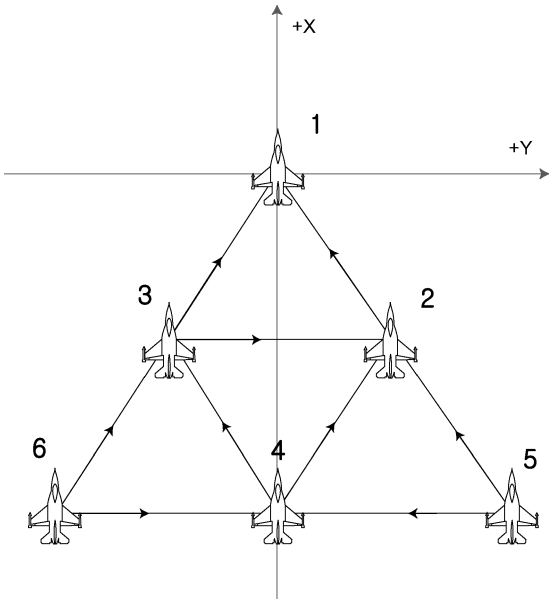

Fig. 8 Six-vehicle formation.

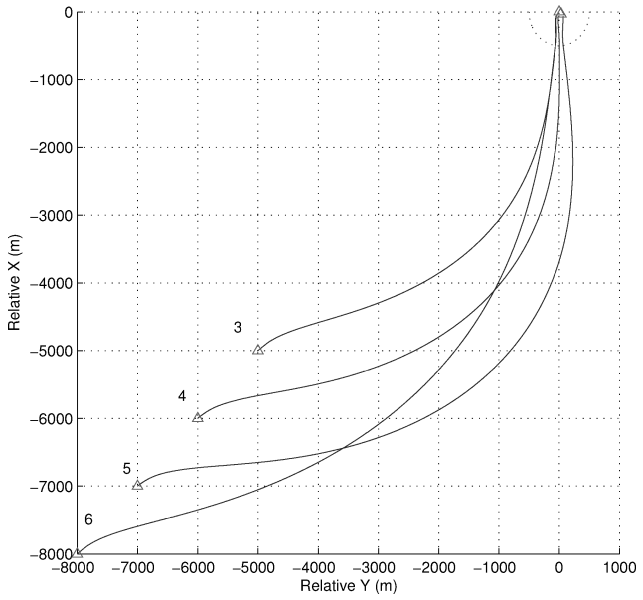

Fig. 9 Case 3: relative $X-Y$.

desired formation position by the guidance law. The θ approach is used on the wingmen until the formation guidance activation region is reached. The commanded angles and target vehicles for the wingmen are given in Table 2.

Figure 8 shows the desired shape of the formation. The direction of the arrow shows which nearby vehicles are considered for $\theta-\theta$ guidance. Vehicle 2 only uses vehicle 1 for $\rho-\theta$ guidance. The simulation is done for 300 s with a time step of 0.1 s. Previous gains used in cases 1 and 2 are used for the θ approach and $\theta-\theta$ guidance law 1. Figure 9 shows the four wingmen approaching with different approach angles to the leader. Figure 10 is the magnified

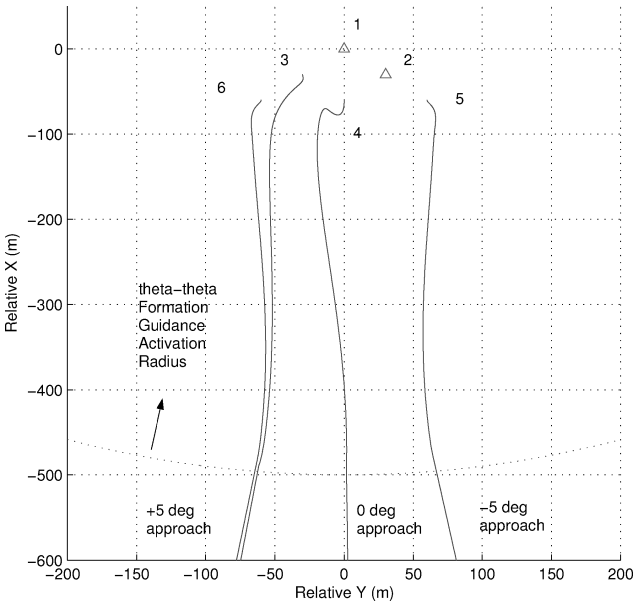

Fig. 10 Case 3: relative $X-Y$ magnified.

view of Fig. 9 near the leader. After passing the formation guidance activation region, each vehicle is guided by the $\theta-\theta$ guidance. We can see that a multiple-vehicle formation can be accomplished by $\theta-\theta$ guidance. Also, by varying the distance and angle between the leader and wingman 1, we can change the total size and shape of the formation.

Conclusions

The main concept of this paper is to use only LOS information for formation flight guidance. Two LOS angles to two nearby vehicles are sufficient when directing a vehicle to a specific location. However, two vehicles in perfect formation are initially required as a basis for other vehicles to join formation. The approach guidance and formation guidance for forming the initial two vehicles are first proposed. For multiple-vehicle formation guidance, two different methods of using the LOS information are proposed. Guidance law 1 uses one angle for flight-path angle command and the other for velocity command. Guidance law 2 uses the sum and difference of LOS angle on both flight-path angle and velocity command. Both are successful in forming a formation with LOS information only. Guidance law 2 has a slightly faster response and settling time but uses more control energy. The stability of the guidance laws is analyzed by finding the Jacobian at the equilibrium point. The formation system stability can be found for specific cases by inputting the formation conditions and gains. The proposed guidance laws are successfully tested on two-vehicle approach and formation simulation, three-vehicle formation simulation, and six-vehicle approach and formation simulation. We have verified that the proposed guidance laws are applicable to multiple-vehicle formation flight. The proposed guidance law will be helpful when a low communication profile is required between the formation vehicles.

References

[1]Hansen, J. L., and Cobleigh, B. R., "Induced Moment Effects of Formation Flight Using Two F/A-18 Aircraft," NASA TM 2002-210732, 2002.

[2]Binetti, P., Ariyur, K. B., Krstic, M., and Bernelli, F., "Formation Flight Optimization Using Extremum Seeking Feedback," *Journal of Guidance, Control, and Dynamics*, Vol. 26, No. 1, 2003, pp. 132–142.

[3]Pachter, M., D'Azzo, J. J., and Proud, A. W., "Tight Formation Flight Control," *Journal of Guidance, Control, and Dynamics*, Vol. 24, No. 2, 2001, pp. 246–254.

[4]Giulietti, F., Pollini, L., and Innocenti, M., "Autonomous Formation Flight," *IEEE Control System Magazine*, Vol. 20, No. 6, 2000, pp. 34–44.

[5]Verma, A., Wu, C. N., and Castelli, V., "Autonomous Command and Control System for UAV Formation," AIAA Paper 2003-5704, Aug. 2003.

[6]Wan, S., Campa, G., Napolitano, M. R., Seanor, B., and Gu, Y., "Design of Formation Control Laws for Research Aircraft Models," AIAA Paper 2003-5730, Aug. 2003.

[7]Li, S. M., Boskovic, J. D., and Mehra, R. K., "Globally Stable Automatic Formation Flight Control in Two Dimensions," AIAA Paper 2001-4046, Aug. 2001.

[8]Pollini, L., Giulietti, F., and Innocenti, M., "Robustness to Communication Failures Within Formation Flight," *Proceedings of the American Control Conference*, American Automatic Control Council, 2002, pp. 2860–2866.

[9]Mehra, R. K., Boskovic, J. D., and Li, S. M., "Autonomous Formation Flying of Multiple UCAVs Under Communication Failure," *Position Location and Navigation Symposium*, Inst. of Electrical and Electronics Engineers, Piscataway, NJ, 2000, pp. 371–378.

[10]Ashokkumar, C. R., and Jeffcoat, D. E., "Cooperative Systems Under Communication Delay," AIAA Paper 2003-5663, Aug. 2003.

[11]Pollini, L., Giulietti, F., and Innocenti, M., "Sensorless Formation Flight," AIAA Paper 2001-4356, Aug. 2001.

[12]Das, A. K., Fierro, R., Kumar, V., Ostrowski, J. P., Spletzer, J., and Taylor, C. J., "A Vision-Based Formation Control Framework," *IEEE Transactions on Robotics and Automation*, Vol. 18, No. 5, 2002, pp. 813–825.

[13]Sattigeri, R., Calise, A. J., and Evers, J. H., "An Adaptive Approach to Vision-Based Formation Control," AIAA Paper 2003-5727, Aug. 2003.

[14]Pollini, L., Mati, R., Innocenti, M., Campa, G., and Napolitano, M., "A Synthetic Environment for Simulation of Vision-Based Formation Flight," AIAA Paper 2003-5376, Aug. 2003.